AAV-Human A53T-Mutated Synuclein Disrupts Nigro-Striatal System in Mice

Ewald Auer, Tina Loeffler, Magdalena Daurer, Livia Breznik, Joerg Neddens, Stefanie Flunkert, Manuela Prokesch

Scantox Neuro GmbH, Grambach, Austria

For further information and inquiries contact office-austria@scantox.com

Background

Phosphorylation, misfolding and aggregation of α-synuclein (α-syn) are hallmarks of Parkinson's disease (PD) and other synucleinopathies. The A53T mutation in the SNCA gene encoding α-syn has been shown to promote oligomerization and aggregation of α-syn, ultimately contributing to neurodegeneration. To evaluate pathological aspects and the efficacy of new treatment strategies for PD, an induced mouse model expressing the A53T-α-syn variant was characterized for its pathology.

Methods

To this end, the substantia nigra (SN) of 13 weeks old C57BL/6J mice was unilaterally injected with AAV-human A53T mutated α-syn (AAV-hA53T). The contralateral SN was treated with an AAV-empty control vector. After 8 weeks, brains were collected. All brains were analyzed for α-syn by MSD immunosorbent assay, AAV2 by fluorescence *in situ* hybridization, hα-syn-pS129, tyrosine hydroxylase (TH), dopamine transporter (DAT), ionized calcium-binding adapter molecule 1 (Iba1), cluster of differentiation (CD) 3, and CD8 by quantitative immunofluorescent labeling. Expression of a panel of novel PD target proteins was assessed by automated western blot (WES).

Results

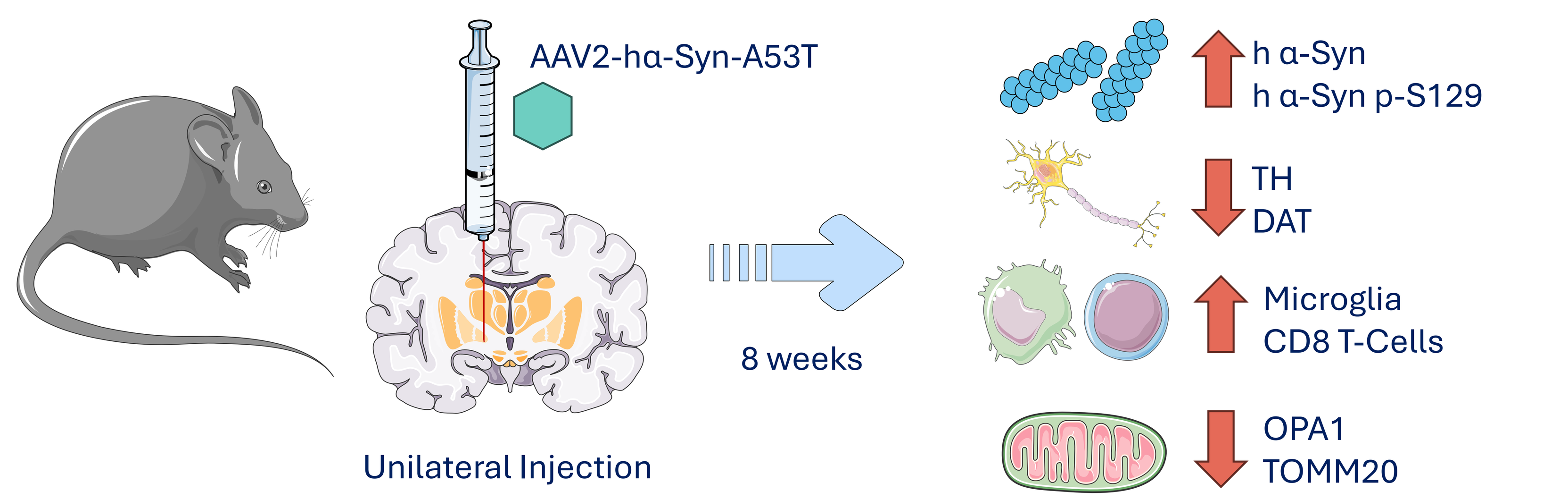

Human α-Synuclein

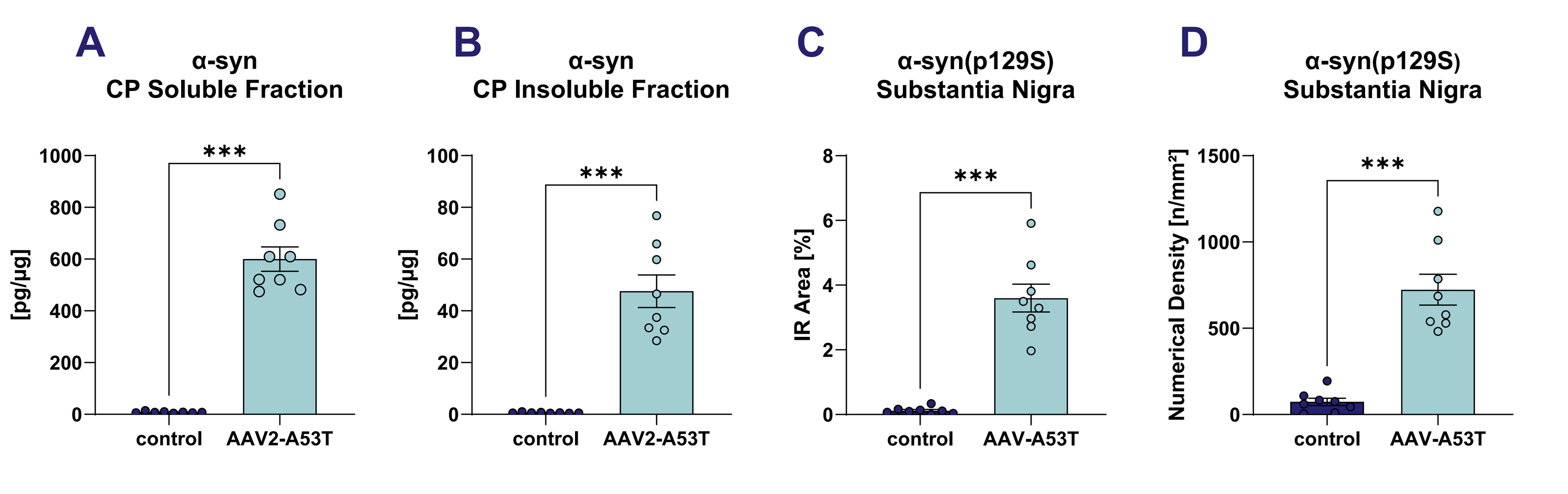

▲ **Figure 1: Increased human α-syn/α-syn(p129S) levels upon unilateral AAV2-hA53T injection. A,B**: Biochemical analysis of human α-syn in the soluble (**A**) and insoluble (**B**) caudate putamen (CP) fraction of AAV2-hA53T-injected brain hemispheres. Mean ± SEM; n = 8 per group. unpaired t-test; ***p <0.001. **C,D:** Immunohistochemical analysis of human α-syn (p129S) in substantia nigra of AAV2-hA53T-injected brain hemispheres, displaying immunoreactive area (**C**) and object density (**D**). Mean ± SEM; n = 8 per group; paired t-test; ***p <0.001.

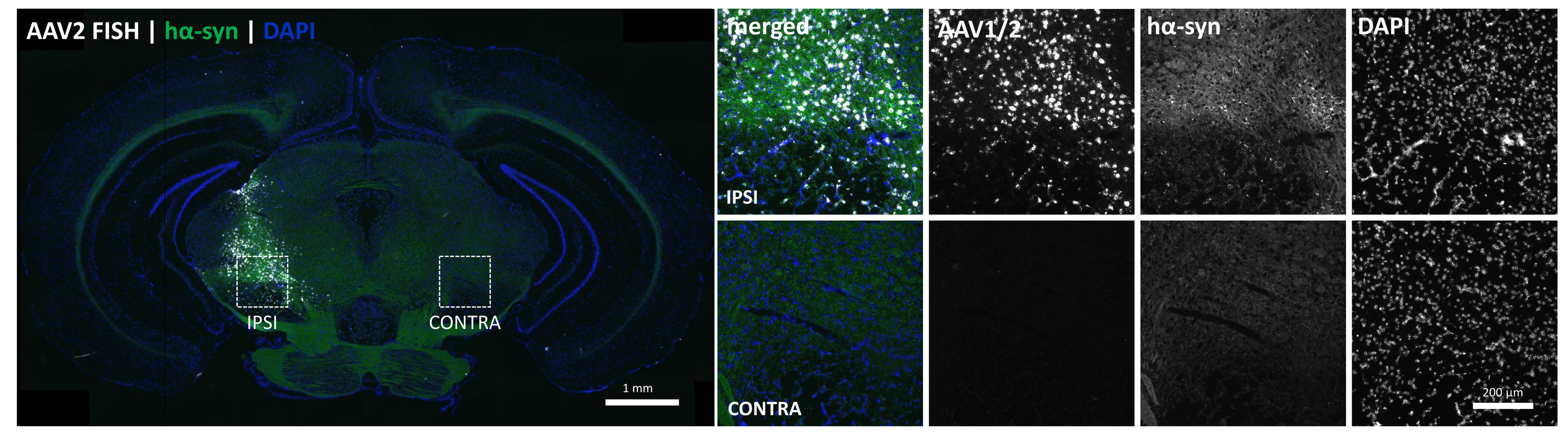

▲ **Figure 2: *In situ* hybridization of AAV2 vector in combination with immunofluorescent labeling of hα-syn protein in an ipsilaterally AAV2-hA53T-injected and contralaterally AAV2-empty vector control-injected mouse brain**. Fluorescent *in situ* hybridization against the AAV2 serotype (white); AAV2 can be observed in the left but not the right hemisphere. Immunofluorescence labeling of hα-syn protein (green) is mostly present close to AAV2 *in situ* labeling. IPSI: ipsilateral hemisphere; CONTRA: contralateral hemisphere. Slides were counterstained with DAPI. Inlets show substantia nigra.

Tyrosine Hydroxylase (TH)

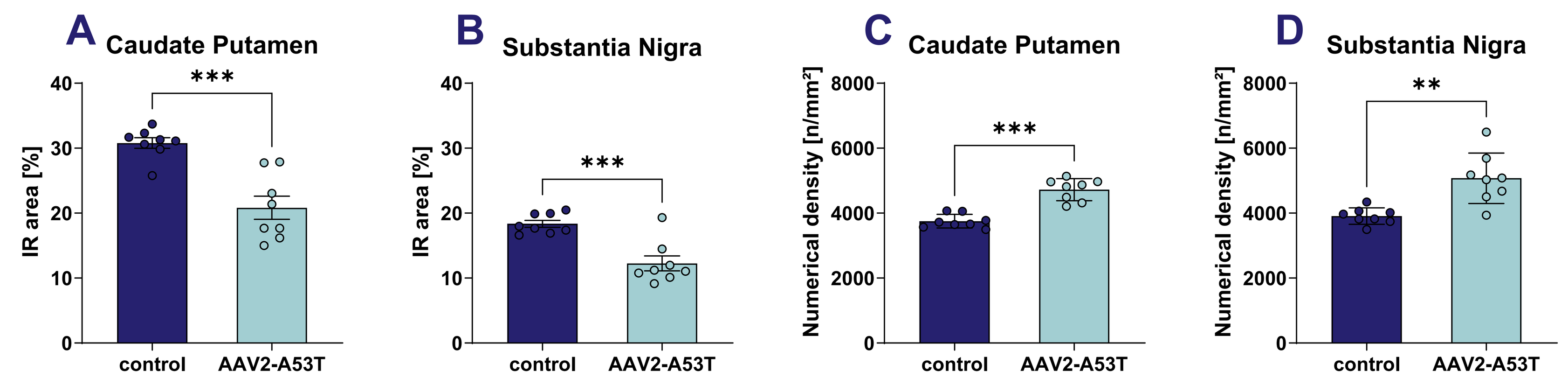

▲ **Figure 3: Loss of TH-positive soma and fibers in the SN and CP indicating a loss of dopaminergic neurons.** Quantification of TH in the caudate putamen and substantia nigra of the AAV2-A53T-injected hemisphere compared to the AAV2-empty vector (control)-injected hemisphere. **A, C:** Caudate putamen. **B, D:** Substantia nigra. **A, B:** Immunoreactive (IR) area in percent. **C, D:** Number of objects as numerical density in n/mm². Mean ± SEM. 5 brain sections per mouse; n = 8 animals per group. Paired t-test. **p <0.01; ***p <0.001.

Dopamine Transporter (DAT)

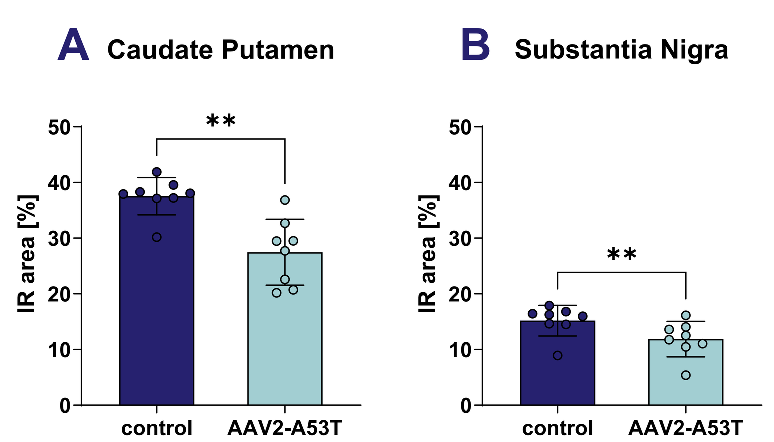

◀ **Figure 4: Reduction of DAT levels upon AAV2-hA53T expression.** Quantification of DAT in the caudate putamen and substantia nigra of the AAV2-A53T-injected hemisphere compared to the AAV2-empty vector (control)-injected hemisphere. **A:** Caudate putamen, **B:** Substantia nigra. Immunoreactive (IR) area in percent. Mean ± SEM. 5 brain sections per mouse; n = 8 animals per group. Wilcoxon matched-pairs signed rank test. **p <0.01.

Activated Microglia

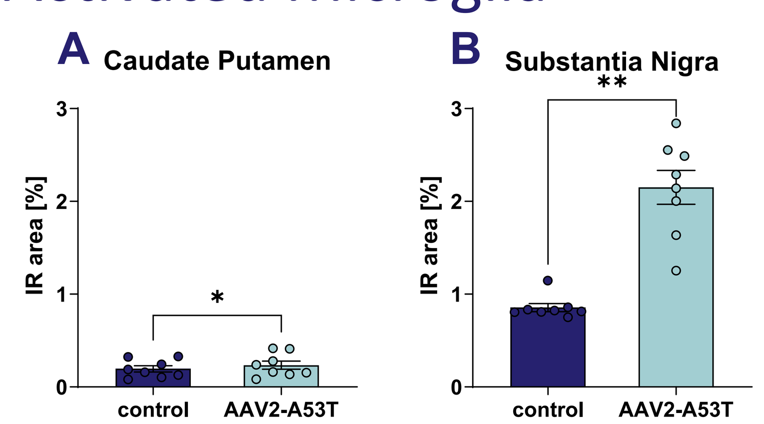

◀ **Figure 5: Microgliosis upon AAV2-hA53T expression.** Quantification of Iba1 in the caudate putamen and substantia nigra of the brain hemisphere injected with AAV2-A53T compared to AAV2-empty vector (control). **A:** Caudate putamen, paired t-test. **B:** Substantia nigra, Wilcoxon matched-pairs signed rank test. Immunoreactive (IR) area in percent. Mean ± SEM. 5 brain sections per mouse; n = 8 animals per group. *p <0.05, **p <0.01.

Infiltration of T-cells

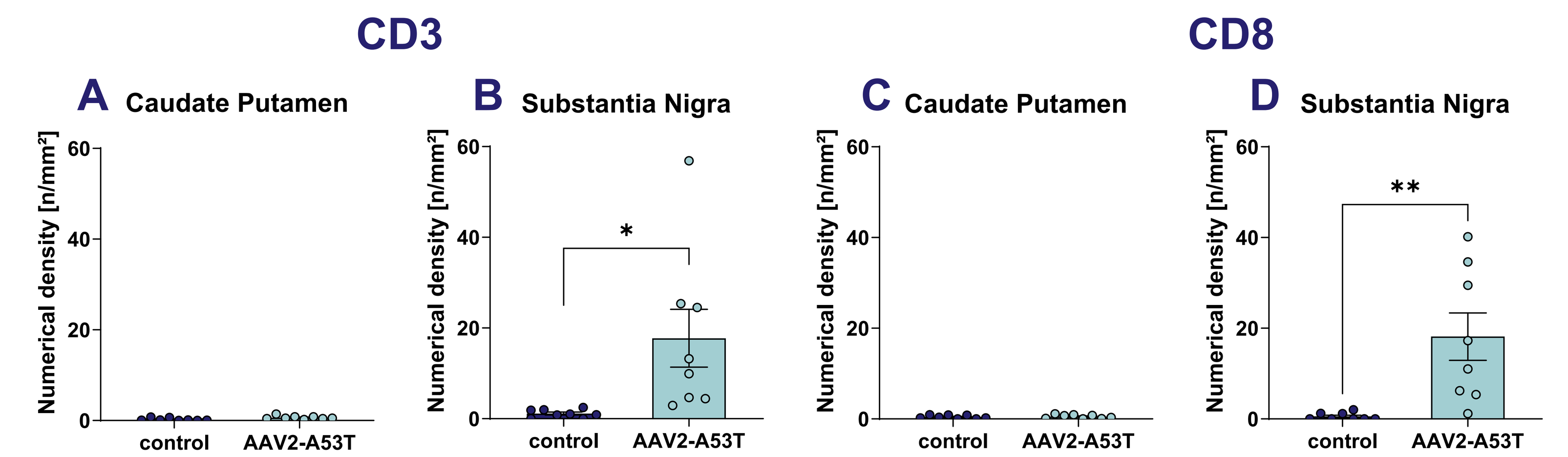

▲ **Figure 6: Infiltration of CD3-positive T-cells, specifically cytotoxic T-cells upon AAV2-hA53T expression. Quantification of CD3- and CD8-positive objects in the caudate putamen and substantia nigra of the AAV2-A53T- injected hemisphere compared to control.** CD3- (**A, B**) and CD8- (**C, D**) positive objects (numerical density) in the caudate putamen (**A, C**) and substantia nigra (**B, D**) of AAV2-A53T-injected hemispheres compared to AAV2-empty vector controls. Mean ± SEM. 5 brain sections per mouse; n = 8 animals per group. Wilcoxon matched-pairs signed rank test (**A, D**) or paired t-test (**B, C**). *p <0.05, **p <0.01.

Mitochondrial PD Markers

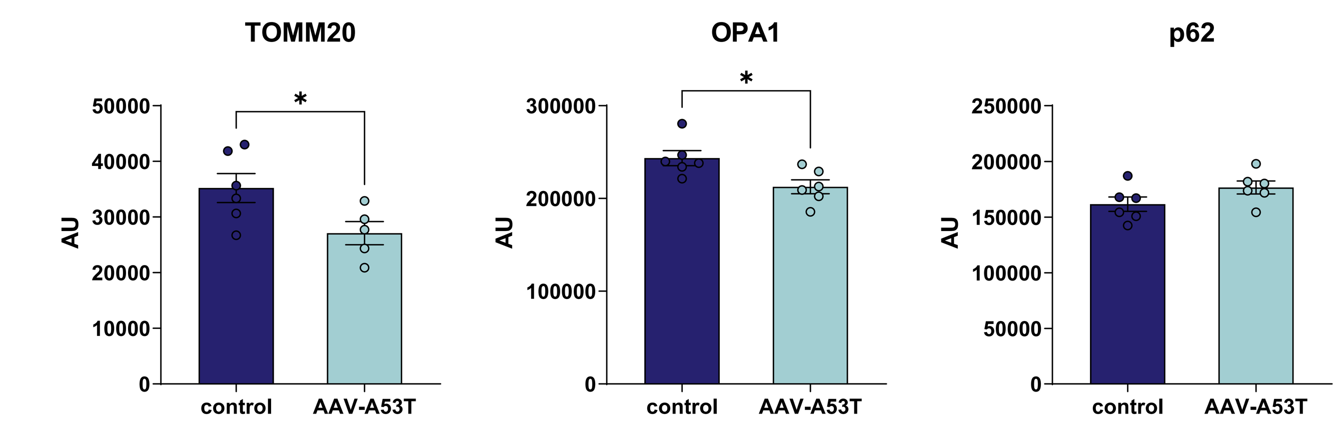

▲ **Figure 7: Decreased levels of mitochondrial proteins TOMM20 and OPA1 upon AAV-A53T expression in striatum, indicating mitochondrial impairment.** Quantification of indicated protein expression in striatum by automated western-blot analysis (protein-simple WES) of AAV2-A53T injected hemisphere compared to AAV2-empty vector injected hemisphere. Mean ± SEM. n = 6 hemispheres per group. Unpaired t-test. *p <0.05.

Conclusion

In summary, the AAV-human A53T α-syn mouse model recapitulates several core features of PD, including increased α-syn phosphorylation, loss of dopaminergic neurons, reduction of dopamine transporter levels – likely associated with loss of dopaminergic terminals, as well as immune activation. Furthermore, expression of mitochondrial PD-associated markers TOMM20 and OPA1 was reduced in this model, while expression of further novel PD-associated proteins p62, NOD2, OGA, TMEM175, TRPML1, and ATP13A2 was readily detectable but unchanged upon hA53T expression (data not shown).

This model allows and enables studying A53T α-syn-related pathologies and downstream signaling and might be further valuable for the analysis of molecular mechanisms underlying synucleinopathies, paving the way for the development of novel therapeutic interventions.